Investigating Particle Size Effects in Catalysis by Applying a Size Controlled and Surfactant-Free Synthesis of Colloidal Nanoparticles in Alkaline Ethylene Glycol – the Case Study of the Oxygen Reduction Reaction on Pt

Jonathan Quinson,[†,‡,*] *Masanori Inaba*,[†,‡] *Sarah Neumann*,[±] *Andreas A. Swane*,[†] *J. Bucher*,[※] *Søren B. Simonsen*,[⁑] *Luise Theil Kuhn*, [⁑] *Jacob. J. K. Kirkensgaard*,[ǂ] *Kirsten M. Ø. Jensen*,[†] *Mehtap Oezaslan*,[ŀ] *Sebastian Kunz*[±] *and Matthias Arenz*[†,※,*]

[†] Department of Chemistry, University of Copenhagen, Universitetsparken 5, DK-2100 Copenhagen Ø, Denmark

[※] Department of Chemistry and Biochemistry, University of Bern, Freiestrasse 3, CH-3012 Bern, Switzerland

[⁑] Department of Energy Conversion and Storage, Technical University of Denmark, Frederiksborgvej 399, 4000 Roskilde, Denmark

[ǂ] Niels Bohr Institute, University of Copenhagen, Universitetsparken 5, 2100 Copenhagen Ø, Denmark

[├] Carl von Ossietzky Universität Oldenburg, School of Mathematics and Science Department of Chemistry, 26111 Oldenburg, Germany

[±] Institute of Applied and Physical Chemistry, University of Bremen, Leobenerstraße, 28359 Bremen, Germany

ABSTRACT

Colloidal platinum nanoparticles are obtained via a surfactant-free polyol process in alkaline ethylene glycol. In this popular synthesis, ethylene glycol functions as solvent and reducing agent. The preparation procedure is known for its reproducibility to obtain 1-2 nm nanoparticles, but at the same time the controlled preparation of larger nanoparticles is challenging. A reliable size control without the use of surfactants is a fundamental yet missing achievement for systematic investigations. In this work it is demonstrated how the molar ratio between NaOH and the platinum precursor determines the final particle size and how this knowledge can be used to prepare and study in a systematic way supported catalysts with defined size and Pt to carbon ratio. Using small-angle X-ray scattering, transmission electron microscopy, infrared spectroscopy, X-ray absorption spectroscopy, pair distribution function and electrochemical analysis it is shown that changing the NaOH/Pt molar ratio from 25 to 3, the Pt nanoparticle size is tuned from 1 to 5 nm. This size range is of interest for various catalytic applications, such as the oxygen reduction reaction (ORR). Supporting the nanoparticles onto a high surface area carbon, we demonstrate how the particle size effect can be studied keeping the Pt to carbon ratio constant, an important aspect that in previous studies could not be accomplished.

KEYWORDS

oxygen reduction reaction, particle size effect, size control, polyol process, platinum nanoparticles, synthesis

INTRODUCTION

Catalysts are essential for many reactions and industrial processes.[1] In particular, precious metal materials have outstanding catalytic properties for energy conversion or chemical production.[2-4] To utilize limited resources efficiently, it is key to optimize precious metal catalysts for specific operation conditions. In many applications, precious metal catalysts consist of nanoparticles ideally finely distributed on a support material. To optimize the catalytic performance of nanoparticles, one needs to individually investigate and optimize various properties like nature of the metal, particle size, support type, metal to support ratio, etc. To best select the most suitable combination of these properties, systematic fundamental research and development of model catalysts must be performed. Since this is a complex multi-parameter challenge, a suitable approach to study and understand the effect of a given property is to control this property independently of the others in a reliable way.

A synthesis method that can address these challenges in the preparation and optimization of precious metal nanoparticles used as catalysts, is based on the 'polyol process'.[5] In the 'polyol process' a metal complex (e.g. H_2PtCl_6) is reduced in an alkaline (e.g. NaOH) solution of polyol

(e.g. ethylene glycol, EG) heated at relatively high temperature (ca. 160 °C). The synthesis recently reviewed[5] is simple and 'green', which accounts for its popularity and an ongoing optimization.[6] To obtain supported nanoparticles, the polyol process is typically performed in a 'one-pot' approach, where precious metals are directly formed on a support.[7] In one-pot syntheses it is often observed that the nature of the support influences the size[8-9] and the effect of particle size cannot be studied independently of the nature of the support, a severe drawback for systematic studies. In the absence of a support, stable colloidal dispersions of precious metal nanoparticles can be obtained. Surfactants such as polyvinylpyrrolidone (PVP) or halides are typically used to stabilize the nanoparticles, avoid agglomeration and tune the particle size.[10] However these surfactants need to be removed before performing catalytic measurements for optimal catalytic activity.[11-14] Surfactant removal requires additional steps and treatment of the supported nanoparticles that can potentially influence nanoparticles and support alike, another drawback for systematic studies.

The surfactant-free polyol synthesis has previously been achieved[15] and is known for its high reproducibility for synthesizing 1-2 nm particles. Based on this synthesis method we developed a surfactant-free 'toolbox' approach of supported catalysts prepared in a two-step synthesis, **Figure 1**.[16] First, a surfactant-free colloidal dispersion that is stable for months[17] and contain precious metal nanoparticles is prepared in alkaline EG. The nanoparticles are precipitated by chemical treatment in acid, re-dispersed, washed, can then be isolated and stored as powder[18] or supported by mixing the desired amount of support material and nanoparticles to achieve a target metal to support ratio.[16, 19] A benefit of the two-step approach is that particle formation and growth is independent of the support. The nanoparticles do not form in parts of the support like pores that are not accessible to the reactants under catalytic operation.[20] Thus, the expensive

material is more efficiently used during catalysis. Another advantage is that high metal contents (> 50 wt. %), beneficial to optimize the stability and the mass activity of catalysts,[21] can be achieved in a single deposition step. Alternative 'one-pot' syntheses of precious metal nanoparticles directly on a support material can require multiple iterations of the synthesis before reaching the desired metal content which leads to undesirable agglomeration of the nanoparticles.[22]

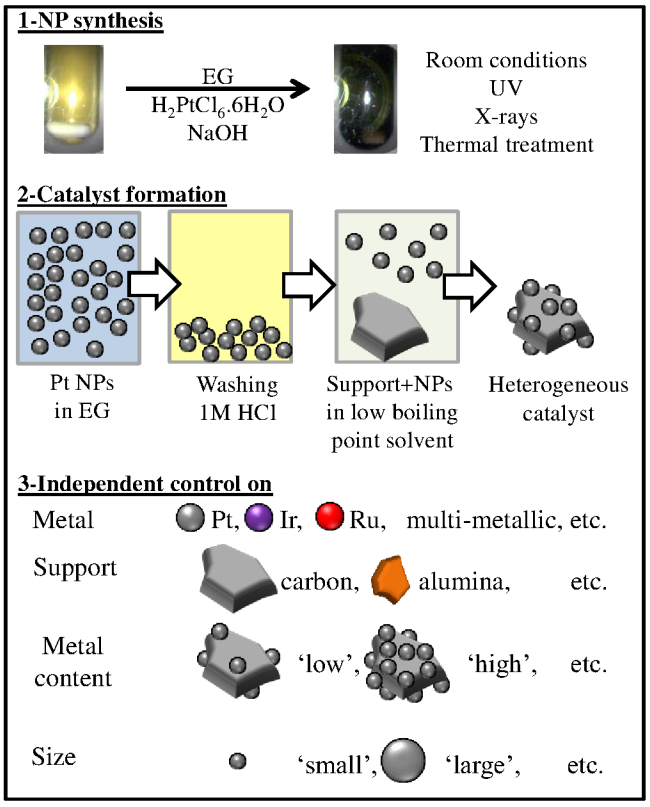

Figure 1. Schematic representation of the steps and ideas to design nanocatalysts by the toolbox approach. (1) Surfactant-free colloidal synthesis of Pt nanoparticles (NPs) in alkaline ethylene glycol (EG). (2) Pt nanoparticles are supported after acidic washing and redispersion in low boiling point solvent. (3) The toolbox approach allows independent control on various

97 experimental parameters for systematic studies and optimization of supported precious metal
98 catalysts.

99 The 'toolbox' approach is suitable to understand and study in a systematic way the influence of
100 the various physical catalyst properties such as the nature of metal, the support, the metal
101 content, the particle size, and inter-particle distance. For this it is essential to be able to change
102 these properties individually, i.e. independent of each other, and to avoid any post-treatment. The
103 toolbox has been successfully exploited to propose routes for improving heterogeneous catalysts
104 in gas sensing,[23] chemical synthesis[18, 24] and electrocatalysis.[16, 25]. For instance, the effect of
105 carbon support, metal content and amount of polymer used in 'ink' formulation were
106 investigated in a comprehensive way for the oxygen reduction reaction (ORR) that plays a key
107 role in fuel cell development.[19, 21, 26] However, a critical missing piece in the toolbox approach
108 was a reliable size control,[27] since at the nanoscale size has a strong influence on catalyst
109 properties like activity, selectivity or stability.[3]

110 Size control in polyol surfactant-free syntheses can be achieved by changing the viscosity of
111 the solvent. For instance, adding water changes the size,[15, 28] but the obtained colloidal
112 dispersions do not lead in our experience to reproducible results without using a protecting
113 polymer. A general agreement is that 'pH' can be used to affect the size of the nanoparticles,
114 with or without the use of polymer, in colloidal or one-pot syntheses, for mono or bimetallic
115 materials.[15, 17, 29-33] It is broadly and commonly stated that 'pH' must be superior to 12 for the
116 reaction to proceed and that 'pH' affects the nanoparticle size.

117 We observed that when the concentration of platinum precursor is increased, size control is
118 more challenging to achieve. This might explain why to the best of our knowledge, the
119 concentration of platinum is kept constant in all studies so far, except one,[34] see also **Table S1**.

Therefore controlling the 'pH' (or NaOH concentration) is not sufficient. In the presented work it is demonstrated by using small-angle X-ray scattering (SAXS), transmission electron microscopy (TEM), infra-red spectroscopy (FTIR), X-ray absorption spectroscopy (XAS), and pair distribution function (PDF) analysis that it is not the 'pH' that controls the size, but the molar ratio between NaOH and platinum. Various samples were prepared with different NaOH/Pt molar ratios using microwave synthesis. It is explained how the nanoparticle size can be tuned in the range 1 to 5 nm when the NaOH/Pt molar ratio is changed from 25 to 3. Particle dispersions with different sizes are then used to prepare supported Pt/C electrocatalysts keeping the metal content constant and to test the influence of particle size on the oxygen reduction reaction (ORR). In previous work[35-36] such investigations were possible only by using complex, multistep preparation protocols employing surfactants that typically need to be removed.[37-38]

RESULTS AND DISCUSSION

NaOH/Pt molar ratio to control platinum nanoparticle size.

In previous efforts to achieve size control in surfactant-free colloidal syntheses of precious metal nanoparticles in alkaline ethylene glycol, pH has been discussed as a crucial parameter.[15]. A strict definition of pH is based on the proton activity in aqueous solution. We therefore refrain from using 'pH' and will prefer to use the 'NaOH concentration'. Yet, it is not always straightforward to reproduce results from the literature. The concentration of precious metal precursors in reported studies is typically in the range 0.5 – 50 mM. The NaOH concentration is typically varied from 0 to 1 M, **Table S1**. Up to now only the effect of the concentration of the base (NaOH or KOH) has been investigated keeping the metal complex concentration constant.[7, 39]

143 The synthesis has recently been performed as a one-pot synthesis including carbon nanotubes
144 as support material.[7] No clear correlation between particle size and electrochemically active
145 surface area (ECSA) was found, indicating a profound influence of the support on the obtained
146 catalyst. In particular the nanoparticle deposition on the support was found to depend on the
147 concentration of NaOH used. The higher the NaOH concentration, the lower the metal content
148 achieved. This is related to the surface charge of the carbon support leading to repulsive
149 interactions with the nanoparticles. This observation stresses the strong influence of the support
150 on the properties of the prepared catalyst in traditional one-pot syntheses, leading in this specific
151 example to a detrimental effect on the achieved metal content. This drawback is completely
152 alleviated in the toolbox approach since synthesis and immobilization are independent steps. In
153 another study, *in-situ* SAXS using synchrotron radiation were used to elucidate the temporal
154 evolution of Pt nanoparticle formation in ethylene glycol, with or without surfactant and for
155 different NaOH concentrations, but at a constant H_2PtCl_6 concentration.[39] However, synchrotron
156 radiation as well as X-ray sources (e.g. from an in-house SAXS equipment) are enough in our
157 experience to induce the formation of the nanoparticles, see also Supporting Information (SI).
158 In the present study, colloidal platinum nanoparticles were synthesized using a microwave
159 reactor and characterized after synthesis to avoid any support or beam-effect during investigation
160 of the nanoparticles. In the microwave reactor-based synthesis reactions can be completed in less
161 than 10 minutes, which enables a high screening output of experimental parameters. The joint
162 influence of the NaOH concentration and the concentration of platinum complex on the resulting
163 size of the platinum nanoparticles is investigated.
164 TEM and SAXS characterization were carried out on colloidal dispersions of Pt nanoparticles
165 prepared by changing the concentration of NaOH for a given H_2PtCl_6 concentration of 10 mM.

Both characterization methods indicate a similar particle size distribution for a given sample, for clarity only the SAXS results are discussed in this first section, **Figure 2** as well as **Table S2** and **Figure S1**. As the concentration of NaOH decreases from 250 mM to 63 mM, the size of the nanoparticles, evaluated as the mode of the fitted size distribution, increases from 1.1 nm to 4.9 nm. The trend observed is that with higher NaOH concentration, the particle size is smaller. This trend agrees with the literature and it is tempting to conclude that the NaOH concentration controls the size.

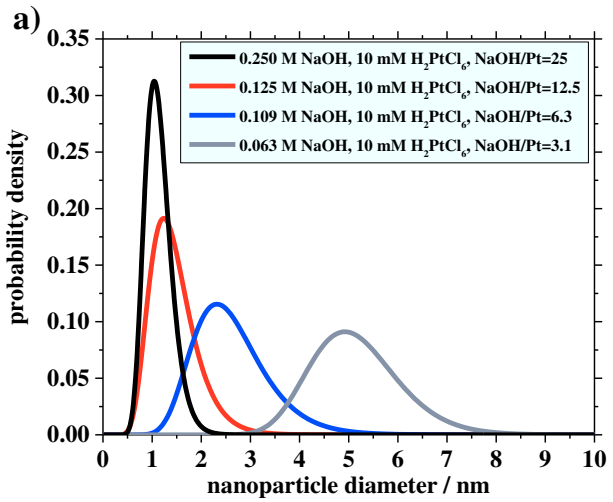

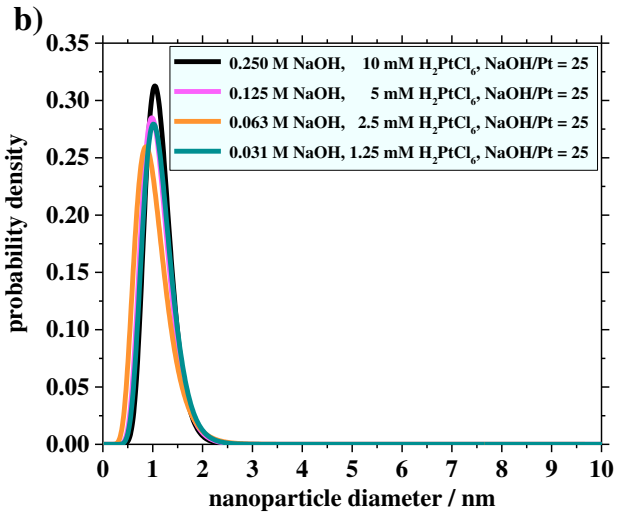

Figure 2. (a) Pt nanoparticle size distribution obtained by SAXS analysis as a function of the concentration of NaOH in the reaction mixture. (b) Pt nanoparticles size distribution obtained by SAXS analysis for different concentration of NaOH and Pt precursor but a same NaOH/Pt molar ratio of 25. Experimental conditions are detailed in the inset.

The used NaOH concentrations translate to a change in the NaOH/Pt molar ratio from 25 to 3.1. To understand the role of the absolute NaOH concentration as compared to the NaOH/Pt molar ratio, we further investigated the case of fixed NaOH/Pt molar ratio but varying the absolute concentrations. For different concentrations of platinum precursor complex, from 2.5 to 20 mM, the NaOH concentration was changed accordingly from 63 mM to 500 mM to obtain a constant NaOH/Pt molar ratio of 25. As demonstrated in **Figure 2b**, in this case, the resulting particle size is for all experiments the same, i.e. around 0.9 - 1.1 nm. The results unambiguously show that the key parameter to control the size of the colloidal platinum nanoparticles is the NaOH/Pt molar ratio and not the absolute NaOH concentration. If the NaOH concentration controls the size, the results obtained for 63 mM NaOH with 10 mM and 2.5 mM H_2PtCl_6 would lead to the same particle size. In contrast, for higher platinum concentration the average particle size is 4.9 nm and for the lower platinum concentration 0.9 nm as demonstrated in our experiments.

The reason for the overlooked assumption in the literature that the 'pH' is key to achieve size control is possibly linked to the pioneering work by Wang et al., who actually investigated the effect of the platinum complex concentration.[15] In their work, no strong effect on the obtained particle size was observed by changing the H_2PtCl_6 concentration from 0.37 mM to 51 mM. This apparently contradicting statement can be resolved by the fact that they 'adjusted the pH' to 12. Since H_2PtCl_6 deprotonates in solution, when higher H_2PtCl_6 concentrations are used, also more

NaOH is needed to balance the acidity of the precursor. Therefore, it can be assumed that in this pioneering work, the authors unaware kept the NaOH/Pt molar ratio close to constant as well. This is why the authors concluded that the method can be used 'in a high metal concentration' and lead to narrow size distribution. We scrutinized the size control by the NaOH/Pt molar ratio in two different laboratories (University of Copenhagen and University of Bremen) and for two different preparation methods (oil bath synthesis and microwave reactor) and found reproducible results showing that the NaOH/Pt molar ratio is a more suitable descriptor than 'absolute NaOH concentration' for size control and more suitable than 'pH', with little meaning in non-aqueous solvent. A possible model to account for this observation is outlined in the SI. In short, estimating the amount of OH^- per Pt surface area of the nanoparticles leads to a similar value for each obtained particle size. Therefore, it can be hypothesized that the ratio of OH^- to Pt surface atoms not only stabilizes the particles in suspension but also controls the particle growth. As a result, the particle size, or more specifically the number of Pt surface atoms of a nanoparticle, depends on the chosen NaOH/Pt ratio.

Physical characterization of nanoparticles with different size

A summary of the characterization of as prepared colloidal Pt nanoparticles obtained with NaOH/Pt molar ratio of 10 and 4.5 by TEM, FTIR, XAS and PDF analysis is given in **Figure 3** and **Table S3**.

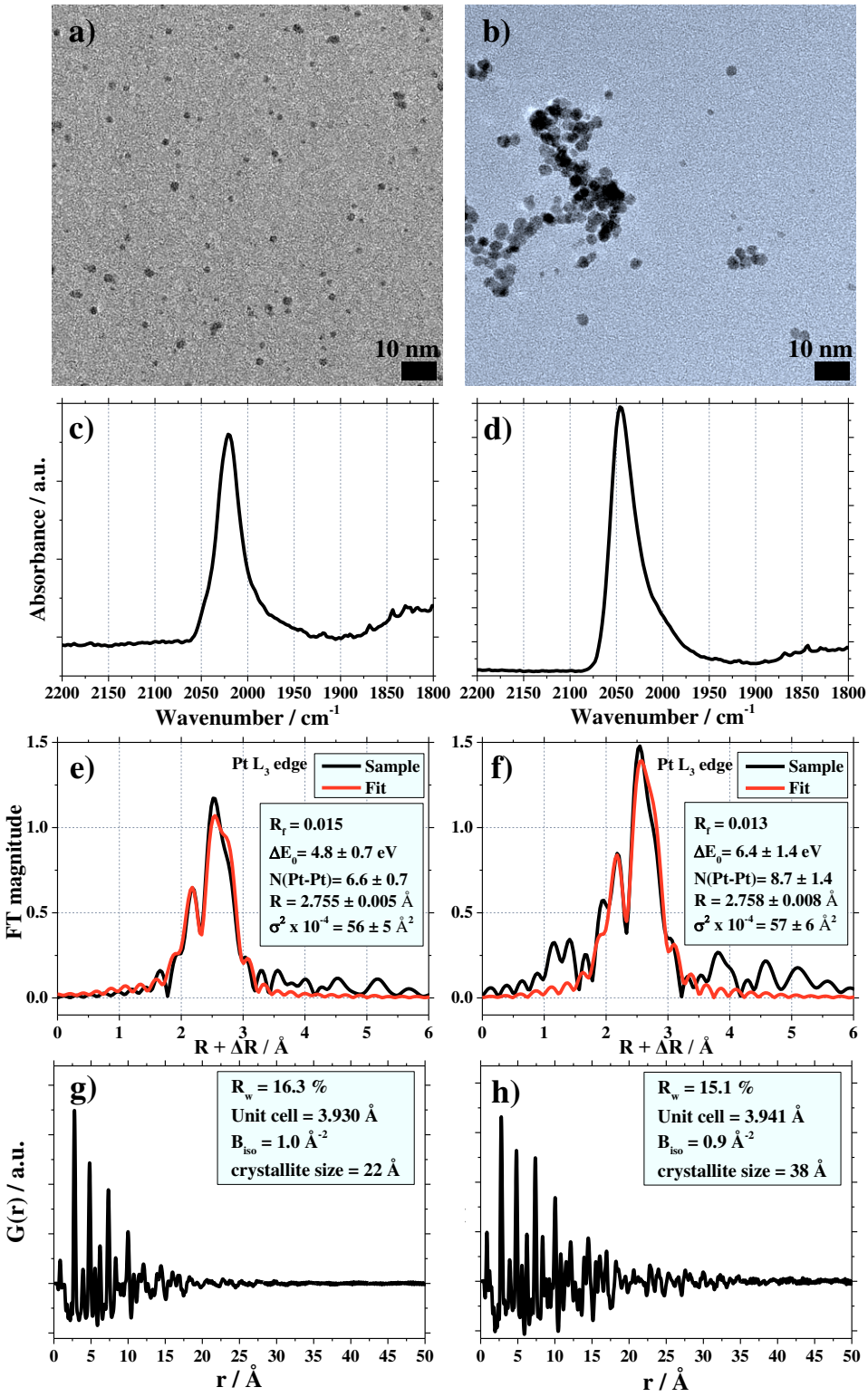

Figure 3. (a,b) TEM, (c,d) FTIR, (e,f) EXAFS for the Pt L_3 edge and (g,h) PDF characterization of Pt nanoparticles prepared with a NaOH/Pt molar ratio of (a,c,e,g) 10 and (b,d,f,h) 4.5.

Based on the TEM analysis, the nanoparticles obtained with a NaOH/Pt molar ratio of 10 exhibit a mean diameter around 2 nm, whereas a NaOH/Pt molar ratio of 4.5 results in diameter in the range 3-5 nm. The TEM data give also indirect evidence of the OH/OH^- stabilization: the 'unprotected nanoparticles' with a larger size, exhibit more agglomeration on the TEM grid than the smaller ones as the surface charge from the OH^- groups protecting them from agglomeration[27] is roughly equal, but larger (heavier) particles need more charge for their stabilization. FTIR characterization reveals an absorption band at 2020 and 2045 cm^{-1} for the smaller and larger nanoparticles, respectively, attributed to CO surface groups on the Pt nanoparticles.[27] The shift to larger wavenumber observed for larger nanoparticles is consistent with previous reports[17, 27] and indicates an increase in CO-CO dipole coupling related to the change in the surface curvature of the particles. X-ray absorption near edge structure (XANES) was used to evaluate the degree of oxidation of the Pt in the colloidal suspension, and extended X-ray absorption fine structure (EXAFS) was used to evaluate the average coordination number and bond distance. It is found that while the initial precursor consists in the form of Pt(IV), after synthesis mainly Pt(0) is detected. Based on Fourier transformed EXAFS data at the Pt L_3 edge, the nanoparticles appear as metallic Pt, suggesting the entire reduction of the Pt(IV) precursor salt after the synthesis. The EXAFS analysis reveals that the atomic length of Pt-Pt bond is around 2.75 Å, whereas the coordination number in the first shell is around 6.6 ± 0.7 and 8.7 ± 1.4 for the nanoparticles prepared with NaOH/Pt molar ratios of 10 and 4.5 respectively. From this analysis, only a rough size estimation can be obtained, but coordination numbers of 6.6 and 8.7 are in agreement with particle sizes of ca. 2 nm and 3-5 nm, respectively.[40-41] PDF analysis, see also **Figure S3-S4**, is a well-suited characterization method to evaluate the atomic structure and the size of crystal domains in nanomaterials.[42-44] The analysis shows that the Pt *fcc* crystal

structure describes the data well for both nanoparticle sizes, and evaluates the crystallite sizes to 2.2 and 3.8 nm for the smaller and larger nanoparticles, respectively. As expected, the refined unit cell parameter is larger for the largest particles.[45] The PDF results therefore agree well with TEM, SAXS and XAS data.

Electrochemical characterization of carbon supported Pt nanoparticles with different sizes

Among the many applications of platinum nanoparticles in heterogeneous catalysis, a surfactant-free synthesis is especially well-suited for electrocatalysis that requires 'clean' catalytic surfaces to ensure efficient electron transfer from/to the catalyst to/from the reactant. One of the main applications of the 'toolbox' approach is therefore the preparation of surfactant-free Pt nanoparticles supported on carbon support (Pt/C) catalysts.[46] The electrochemical properties of carbon supported Pt/C catalysts prepared with a nominal Pt content of 50 wt. % and Pt nanoparticles of different size are summarized in **Figure 4** and **Table 1**. In the cyclic voltammograms (CVs) of all Pt/C catalysts, the typical features of platinum are observed, i.e. the CVs divide into three main regions: the hydrogen underpotential deposition (H_{upd}) region between 0.05 and 0.35 V (all voltages are expressed versus the reversible hydrogen electrode, RHE), the 'double layer' potential region between 0.35 and 0.7 V where mainly capacitive processes take places, and the 'oxide region' above 0.7 V, where OH adsorption and oxide formation on the Pt surface occurs.

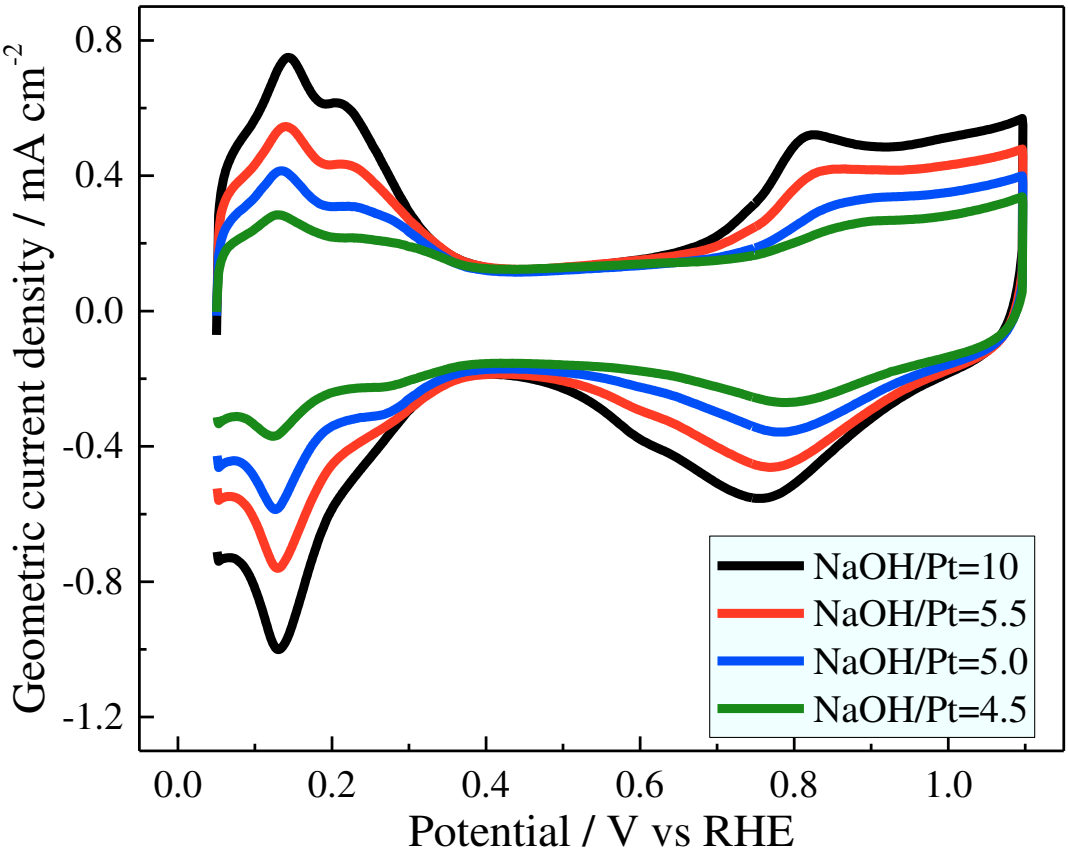

Figure 4. CVs for Pt/C catalysts prepared from different colloidal Pt particle suspensions. The Pt to carbon ratio in the catalyst and the amount of Pt on the glassy carbon were kept constant at 50 wt. % and 14 $\mu g_{(Pt)}$ cm^{-2}, respectively. The measurements were conducted in Ar-saturated 0.1 M $HClO_4$ at a scan rate of 50 mV s^{-1}.

The CVs of the Pt/C catalysts prepared from the different colloids exhibit an increase in the observed H_{upd} area with increasing NaOH/Pt molar ratio during synthesis. Because the same Pt loading on the GC tip was used for each CV, the observed trend shows that the electrochemical active surface area (ECSA) increases with increasing NaOH/Pt molar ratio. As ECSA and particle size are correlated with each other, this is expected. The NaOH/Pt molar ratio ultimately influences the electrochemical properties of the nanoparticles. This is also seen by the shift in the peak potential of the oxide reduction

peak around 0.8 V. A higher NaOH/Pt molar ratio, and thus smaller Pt particle size, leads to a shift of the oxide reduction peak to lower potentials and can be explained by the higher oxophilicity of smaller Pt nanoparticles.[47] This is in agreement with ORR tests summarized in **Table 1** (see also **Figure S5-S8**).

It is worth pointing out that several reports using a one-step synthesis of carbon supported Pt nanoparticles stress the influence of the 'pH' on the maximum metal content achieved.[7, 48-49] As demonstrated, using the presented synthesis approach, the Pt to carbon ratio in the catalyst and the Pt size are controlled independently and the particle size effect[35-36, 50] can be investigated at constant Pt content in the catalyst. Keeping the Pt to carbon support ratio constant but varying the particle size a clear trend in electrochemical surface area (ECSA), specific activity (SA) and mass activity (MA) is observed: with increasing particle size, the SA slightly increases, but the ECSA decreases more significant, resulting in an overall decrease in MA. This study confirms the particle size effect on the ORR discussed in previous reports, i.e. that the SA increases with particle size. Here, for the first time the metal content in the catalyst is kept constant, and only the particle size is varied. Previous studies changed particle size and metal content at the same time.[35-36, 50] Our results indicate that initially reported relatively low SA values at very small particle size (or very high ECSA) in the work of Gasteiger et al.[36] might be related to the use of relative low metal to carbon ratio and resulting higher capacitive current contributions. Low metal to carbon ratio to achieve high ECSA values is a direct consequence of practical limitations in the catalyst preparation that are overcome in the approach presented. Thus, the significance of the particle size effect for the ORR was previously overestimated. Changing the particle size from 2 nm to more than 5 nm at constant metal loading, increases the SA by less

297 than 50 %, and is therefore clearly overcompensated by the concurrent significant increase in
298 ECSA.

299 In addition, the MA obtained with our home-made catalysts is ca. 37 % higher than for a
300 commercial catalysts (TKK) with a similar nanoparticle size (2 nm) and loading (ca. 50 wt. %).
301 This can be attributed to the improved control over catalyst optimization approach using the
302 presented tool-box approach. Our results therefore highlight the benefits of the approach to study
303 and optimize supported catalysts.

304

305 **Table 1**. ECSA and ORR activity values for homemade and commercial Pt catalysts
306 supported on carbon.

NaOH/Pt	Diameter [nm]	ECSA [$m^2\ g^{-1}_{Pt}$]	SA [$mA\ cm^{-2}$]	MA [$A\ g^{-1}_{Pt}$]
TKK	2.2 ± 0.6	93 ± 7	0.74 ± 0.07	680 ± 70
10	2.1 ± 0.6	102 ± 8	0.90 ± 0.18	922 ± 223
5.5	2.9 ± 0.9	84 ± 2	0.92 ± 0.06	778 ± 37
5	4.0 ± 1.2	54 ± 3	1.06 ± 0.08	570 ± 10
4.5	5.5 ± 1.6	38 ± 1	1.20 ± 0.19	457 ± 52

307 ECSA: electrochemically active surface area, SA: specific activity @ 0.9 V; MA: mass activity
308 @ 0.9 V. All Pt/C catalyst are prepared with a nominal Pt loading of 50 wt.%. ECSA, SA and
309 MA were evaluated from at least three independent experiments and calculated with respect to
310 the actual Pt content. The particle diameter is estimated by TEM analysis.

CONCLUSIONS

A straightforward control over the size of Pt nanoparticles prepared via the popular alkaline polyol method is achieved by varying the molar ratio of NaOH/Pt molar ratio used during the synthesis. Nanoparticles with controlled size in the range 1-5 nm were successfully obtained using NaOH/Pt ratios between 25 and 3 and characterized by TEM, SAXS, XAS, FTIR, PDF as well as electrochemical measurements. The characterization confirms that not the 'pH', but the NaOH/Pt molar ratio controls particle size and thus the properties of the as-prepared catalysts. We hypothesize that the concentration of surface species (in our case OH/OH^-) controls not only the stabilization but also the end of the growth process. The presented finding is an important addition to the toolbox approach since all fundamental properties of supported catalysts, i.e. particle size, metal loading, support type, etc. can be now independently controlled and tuned for specific applications. In particular, it is demonstrated how specific activity, electrochemical active surface area, and mass activity of the ORR are influenced by the particle size of Pt at constant metal loading. Compared to previous investigations[35-36, 50], the significance of the particle size effect on the ORR is significantly smaller in the present study, which can be explained by the fact that previously catalysts with different Pt loadings were compared, i.e. multiple parameters were changed at the same time.

EXPERIMENTAL SECTION

Polyol synthesis. For the synthesis of the nanoparticles the polyol synthesis was used.[15, 51-53] The general procedure for a microwave reactor synthesis is detailed.

To obtain ca. 2 nm size Pt nanoparticles: 4 mL of a solution of NaOH (98.9%, Fisher Chemical) at 0.4 M in ethylene glycol (EG, 99.8%, Sigma-Aldrich) with an equal volume of a solution of Pt salt $H_2PtCl_6.6H_2O$ (99,9 % Alfa Aesar) at 40 mM in EG are placed in a micro wave reaction vessel. The NaOH/Pt molar ratio is then 10 for a H_2PtCl_6 concentration of 20 mM in 8 mL. The mixture is heated up 3 minutes at 160 °C with a micro-wave reactor (CEM Discover SP) using a power of 100 W.

To obtain ca 4 nm size Pt nanoparticles: 4 mL of a solution of NaOH at 90 mM in EG with an equal volume of a solution of Pt salt $H_2PtCl_6.6H_2O$ at 20 mM in EG are placed in a microwave reaction vessel. The NaOH/Pt ratio is then 4.5 for a H_2PtCl_6 concentration of 10 mM in 8 mL. The mixture is heated up 3 minutes at 160 °C.

Unless otherwise specified in the text of Figure captions, the nanoparticles are obtained following the general procedure: 20 mM H_2PtCl_6 in 8 mL of alkaline EG for a synthesis time of 3 minutes at 160 °C and for various NaOH/Pt molar ratio.

The general procedure to obtain nanoparticles with the oil bath synthesis is to carry out the reaction using an organic oil bath preheated to 160 °C. The Pt and NaOH solution are then added to a round bottomed ask and submerged with stirring in the oil bath. After approximately 5 minutes, the solution turns dark, like in the microwave synthesis, and the colloidal suspension is heated for another 85 minutes to ensure all the Pt has been reduced.

Pt nanoparticles washing and immobilization on carbon. To collect the particles an aqueous solution (Milli-Q, Millipore, 18.2 MΩ.cm) ca. 30 mL of 1 M HCl (prepared

356 from 30 % HCl Suprapur®, EMD Millipore, Merck KGaA) is added to 7.3 mL of the Pt
357 nanoparticles in EG. The mixture is centrifuged at 2400 relative centrifugal force (4000
358 rotations per minute, Sigma 2-5) for 5 minutes. The nanoparticles can then be collected
359 since they are not a stable colloidal dispersion anymore. The washing/centrifugation with
360 1 M HCl in Milli-Q water is performed 3 times. The nanoparticles are re-dispersed in 7
361 mL of acetone (technical grade) and a desired mass of carbon black is added (Vulcan
362 XC72R, Cabot Corporation) so that the Pt/C ratio is equal to 50 wt. %. By simply
363 sonicating the mixture with an ultrasonic bath (VWR ultrasonic cleaner) for 1 hour the
364 acetone evaporate and the dried powder of Pt nanoparticles supported on carbon is
365 obtained. The powder is re-dispersed into water and the dispersion sonicated for 10
366 minutes. The powder is then filtered and washed with Milli-Q water.

367 The obtained Pt/C ratio was controlled by an indirect Pt proof (IPP). In short, a part of
368 the respective Pt/C sample (typically around 1 - 2 mg) is weighed and transferred to a
369 glass tube, where the carbon is carefully burned off with a gas burner. To digest the Pt,
370 0.5 mL of aqua regia (mixture of 37 % HCl and 65 % HNO_3 in a volume ratio of 1:0.206) is
371 added and heated in a water bath at ca. 60 °C for 2 h. Thereafter, ca. 5 – 10 ml of deionized (DI)
372 water are added and the pH is adjusted to a value of 6.8 – 7.0 controlled by a pH meter. Finally,
373 the sample volume is expanded to 25 mL. The Pt concentration is determined by an IPP method,
374 which has been confirmed with Pt calibration solutions and by comparison to commercial Pt/C
375 samples as well as standard ICP-MS analysis. For the IPP method, a spatula of copper powder
376 and a small piece of the Pt bulk material is added to the prepared aqua regia sample and stirred
377 for 10 minutes at room temperature. Thereafter the solution is filtrated to separate the solids from
378 the liquids and 1 mL of the filtrate is mixed with 2 mL DI-water and two drops of 0.25 M HCl as

well as a spatula of a Murexid/NaCl mixture. Finally, the pH is adjusted to pH to 8 - 10 by adding 1 M NH_3 (colour should change to yellow) and the prepared sample is titrated against 0.1 mM ethylene diamin tetra acidic acid (EDTA). For each sample 10 titrations are performed to give a reliable average.

SAXS characterization. The as-prepared colloidal suspensions were placed in quartz capillaries for SAXS measurements. The measurements and subsequent modelling to extract particle size distribution were performed as previously described[16, 19, 27] and detailed in SI using a SAXSLab instrument installed at the Niels Bohr Institute of the University of Copenhagen.

TEM characterization. For TEM analysis of the as produced colloidal solution a Jeol 2100 microscopes operated at 200 kV was used. To characterize the supported catalyst on carbon, a FEI Tecnai Spirit microscope operated at 80 kV was used. The size analysis was performed by measuring the size of typically 300 (at least 180) nanoparticles and samples characterized by taking images of (at least) 3 different magnifications in (at least) 5 different areas of the TEM grids. The TEM grids were prepared by dropping the solutions of nanoparticles re-dispersed in acetone or the ink re-dispersed in isopropanol:Milli-Q (1:3, v:v) on carbon support films on Cu 300 mesh grids (Quantifoil). The *ImageJ* software was used to measure the nanoparticle sizes and the nanoparticles counted manually (without automated processing of the image). For each sample obtained under different experimental conditions, the mean value of the particle size was used to estimate the average diameter of the nanoparticles, the deviations reported correspond to the standard deviation.

FTIR characterization. The as-synthesized colloidal dispersions in alkaline EG were placed in a cell allowing to record IR spectra of liquid sample in an attenuated total reflectance mode by FTIR spectroscopy. Infrared spectra were captured using a Nicolet 6700 FT-IR (Thermo Electra Corporation) with a zinc selenite prism. All spectra were recorded with a resolution of 4 cm^{-1} and averaging over 100 scans. A background spectrum of EG was measured and subtracted to the spectra recorded for the colloidal suspension. Only the difference spectra are reported.

XAS (EXAFS/XANES). XAS measurements were performed at the B18 beamline at the Diamond Light Source (DLS), UK. The storage ring of the DLS was operated at a beam current of 300 and 400 mA, respectively, and the storage ring energies were 3.0 and 2.4 GeV, respectively. The Pt L_3 edge XAS spectra were recorded in fluorescence mode by using a 9 element Ge solid state detector system. The averaged XAS spectra were then analyzed by using the IFEFFIT software suite.[54] All spectra were background subtracted and normalized. The energy units (eV) were converted to photoelectron wave vector k units ($Å^{-1}$) by assigning the photoelectron energy origin, E_0, corresponding to k = 0, to the first inflection point of the absorption edge. The resulting $\chi(k)$ functions were weighted with k^2 to compensate for the dampening of the XAFS amplitude with increasing k. The resulting EXAFS spectra then were Fourier-transformed to obtain pseudo radial structure functions (RSFs).

To estimate the amplitude reduction factor (S_0^2), a Pt foil was used as reference. The coordination number (N), interatomic bond length (R), mean squared bond length disorder (σ^2) and correction to the energy origin (ΔE_0), together with their error bars were established for each sample by fitting theoretical EXAFS signal to the data in r-space. The

R_f factor reported indicates the closeness of the fit to the data as quality parameter. The linear fit combination method was carried out to establish the oxidation of Pt ions in the liquid by using the respective XANES spectra from K_2PtCl_4 (99.9 % Alfa Aesar), K_2PtCl_6 (99.9 % Alfa Aesar) and Pt foil.

The samples used were characterized as-synthesized and after washing with HCl before redispersion in EG. No strong differences could be observed between the samples before or after washing.

PDF characterization. X-ray total scattering data were collected at beamline P02.1, PETRAIII, DESY using an X-ray wavelength of 0.2072 Å, and a Perkin-Elmer amorphous silicon detector (40 by 40 cm) at a detector distance of 20.059 cm. The samples were loaded in 1 mm kapton tubes. Data was collected for each sample for 12 minutes. The nanoparticles were washed in HCl as described above and redispersed in ethylene glycol (concentration of 2 mM) for the measurements. Ethylene glycol was used as background. The data were integrated using *Fit2D*[55] and Fourier transformed in *xPDF* suite.[56] To extract quantitative information, the PDFs were modeled using *Diffpy-CMI*.[57] The PDFs were modelled applying the *fcc* structure (spacegroup *Fd-3m*) and a spherical dampening function, describing the crystallite size. The data analysis is described further in **Supporting Information**.

Electrochemical characterization. The electrochemical measurements were performed using a home-built potentiostat and a rotating disk electrode (RDE) setup. The electrochemical cell was a home-built Teflon cell based on a three-compartment configuration. A platinum mesh and a saturated calomel electrode (Schott) were used as a counter electrode and a reference electrode, respectively. All potentials in this work are referred to the reversible hydrogen electrode (RHE) potential, which was experimentally

447 determined for each measurement series. 0.1 M $HClO_4$ was prepared as electrolyte with
448 70 % $HClO_4$ (Merck, suprapur) and Milli-Q water.
449 Prior to the RDE measurements, a glassy carbon (GC) disc electrodes (5 mm in
450 diameter) was polished to mirror finish using alumina oxide paste 0.3 and 0.05 μm
451 (Struers, AP-D and AP-A suspension), and cleaned ultrasonically in Milli-Q water.
452 Catalyst ink was prepared by mixing typically 5.5 mg catalyst powder with 7.5 mL Milli-
453 Q water and 2.5 mL isopropanol (IPA, 99.7+ %, Alfa Aesar). A few μl of 1M KOH
454 solution was also added to the ink so that pH of the ink is between 10 and 11. The glass
455 vial containing catalyst ink was sonicated for 15 minutes. A 10 μL aliquot of the ink was
456 pipetted onto the GC electrode leading to a Pt loading of 14 μg_{Pt} cm^{-2}, and thereafter dried
457 in IPA atmosphere at room temperature.[51]
458 All electrochemical measurements were performed in 0.1 M $HClO_4$ solution at 20 °C.
459 The solution resistance between the working electrode and the Luggin capillary was
460 determined using an AC signal (5 kHz, 5 mV) and thereafter compensated for using the
461 potentiostat´s analog positive feedback scheme. The resulting effective solution resistance
462 was less than 3 Ω for each experiment. Prior to the measurements the electrolyte was de-
463 aerated by purging with Ar gas (99.998%, Air Liquide), and the measurements were
464 started with cleaning the catalyst by potential cycles between 0.05 and 1.2 V at a scan rate
465 of 500 mV s^{-1}.
466 Electrochemical surface area (ECSA) of the catalyst was determined from CO stripping
467 charge recorded at a scan rate of 50 mV s^{-1} and conversion coefficient of 396 μC cm^{-2}.
468 Catalytic activity for oxygen reduction reaction (ORR) was determined from positive
469 going polarization curves recorded in O_2 saturated electrolyte at a scan rate of 50 mV s^{-1}

and a rotation speed of 1600 rpm. The polarization curves were corrected for the nonfaradaic background by subtracting the cyclic voltammograms (CVs) recorded in Ar-purged electrolyte.

ASSOCIATED CONTENT

Supporting Information.

The following files are available free of charge.

Literature summary on size control in surfactant-free polyol synthesis of platinum nanoparticles, SAXS, characterization of nanoparticles obtained with different NaOH/Pt molar ratio, PDF, TEM, electrochemical data (PDF)

AUTHOR INFORMATION

Corresponding Authors

* E-mails: matthias.arenz@dcb.unibe.ch, jonathan.quinson@chem.ku.dk

ORCID

Matthias Arenz: 0000-0001-9765-4315

Jonathan Quinson: 0000-0002-9374-9330

Author Contributions

The manuscript was written through contributions of all authors. All authors have given approval to the final version of the manuscript. ‡These authors contributed equally.

ACKNOWLEDGMENT

M.A. acknowledges the support from the Villum Foundation in form of a block stipend. J.Q. has received funding from the European Union's Horizon 2020 research and innovation program under the Marie Skłodowska-Curie grant agreement No 703366 (SELECTRON). M.I. acknowledges the support of Toyota Central R&D Labs., Inc. K.J. acknowledges funding from the Danish Research Council under the Sapere Aude research Talent Program. Diamond Light Source, Hartwell, UK is thanked - in particular Dr Giannantonio Cibin and Ann-Kathrin Geiger - for access to synchrotron beamline B18 (proposal SP12746) that contributed to the results presented. We acknowledge beamtime granted at beamline P02.1, PETRAIII, DESY, a member of the Helmholtz Association (HGF). We would like to thank Martin Etter for assistance in the PDF measurements. S.K. gratefully acknowledges the "Fonds der Chemischen Industrie" (FCI) for financial support through a Liebig Research Grant.

REFERENCES

1. Olveira, S.; Forster, S. P.; Seeger, S. Nanocatalysis: Academic Discipline and Industrial Realities. *J. Nanotechnol.* **2014,** *Article ID 324089*.

2. Rai, M.; Ingle, A. P.; Birla, S.; Yadav, A.; Dos Santos, C. A. Strategic Role of Selected Noble Metal Nanoparticles in Medicine. *Crit. Rev. Microbiol.* **2016**, *42*, 696-719.

3. Antolini, E. Structural Parameters of Supported Fuel Cell Catalysts: The Effect of Particle Size, Inter-Particle Distance and Metal Loading on Catalytic Activity and Fuel Cell Performance. *Appl. Catal., B* **2016**, *181*, 298-313.

4. Chen, C. W.; Tano, D.; Akashi, M. Colloidal Platinum Nanoparticles Stabilized by Vinyl Polymers with Amide Side Chains: Dispersion Stability and Catalytic Activity in Aqueous Electrolyte Solutions. *J. Colloid Interface Sci.* **2000**, *225*, 349-358.

5. Dong, H.; Chen, Y. C.; Feldmann, C. Polyol Synthesis of Nanoparticles: Status and Options Regarding Metals, Oxides, Chalcogenides, and Non-Metal Elements. *Green Chem.* **2015**, *17*, 4107-4132.

6. Alekseenko, A. A.; Ashihina, E. A.; Shpanko, S. P.; Volochaev, V. A.; Safronenko, O. I.; Guterman, V. E. Application of CO Atmosphere in the Liquid Phase Synthesis as a Universal Way to Control the Microstructure and Electrochemical Performance of Pt/C Electrocatalysts. *Appl. Catal., B* **2018**, *226*, 608-615.

7. Aoun, N.; Schlange, A.; dos Santos, A. R.; Kunz, U.; Turek, T. Effect of the OH-/Pt Ratio During Polyol Synthesis on Metal Loading and Particle Size in DMFC Catalysts. *Electrocatalysis* **2016**, *7*, 13-21.

8. Liu, J.; Liu, C. T.; Zhao, L.; Zhang, J. J.; Zhang, L. M.; Wang, Z. B. Effect of Different Structures of Carbon Supports for Cathode Catalyst on Performance of Direct Methanol Fuel Cell. *Int. J. Hydrogen Energy* **2016**, *41*, 1859-1870.

9. Qin, Y. H.; Yang, H. H.; Zhang, X. S.; Li, P.; Ma, C. A. Effect of Carbon Nanofibers Microstructure on Electrocatalytic Activities of Pd Electrocatalysts for Ethanol Oxidation in Alkaline Medium. *Int. J. Hydrogen Energy* **2010**, *35*, 7667-7674.

10. Cookson, J. The Preparation of Palladium Nanoparticles. *Platinum Met. Rev.* **2012**, *56*, 83-98.

11. Park, J. Y.; Aliaga, C.; Renzas, J. R.; Lee, H.; Somorjai, G. A. The Role of Organic Capping Layers of Platinum Nanoparticles in Catalytic Activity of CO Oxidation. *Catal. Lett.* **2009**, *129*, 1-6.

12. Naresh, N.; Wasim, F. G. S.; Ladewig, B. P.; Neergat, M. Removal of Surfactant and Capping Agent from Pd Nanocubes (Pd-NCs) Using Tert-butylamine: its Effect on Electrochemical Characteristics. *J. Mater. Chem. A* **2013**, *1*, 8553-8559.

13. Safo, I. A.; Oezaslan, M. Electrochemical Cleaning of Polyvinylpyrrolidone-capped Pt Nanocubes for the Oxygen Reduction Reaction. *Electrochim. Acta* **2017**, *241*, 544-552.

14. Li, D. G.; Wang, C.; Tripkovic, D.; Sun, S. H.; Markovic, N. M.; Stamenkovic, V. R. Surfactant Removal for Colloidal Nanoparticles from Solution Synthesis: The Effect on Catalytic Performance. *ACS Catal.* **2012**, *2*, 1358-1362.

15. Wang, Y.; Ren, J. W.; Deng, K.; Gui, L. L.; Tang, Y. Q. Preparation of Tractable Platinum, Rhodium, and Ruthenium Nanoclusters with Small Particle Size in Organic Media. *Chem. Mater.* **2000**, *12*, 1622-1627.

16. Speder, J.; Altmann, L.; Roefzaad, M.; Baumer, M.; Kirkensgaard, J. J. K.; Mortensen, K.; Arenz, M. Pt Based PEMFC Catalysts Prepared from Colloidal Particle Suspensions - a Toolbox for Model Studies. *Phys. Chem. Chem. Phys.* **2013**, *15*, 3602-3608.

17. Baranova, E. A.; Bock, C.; Ilin, D.; Wang, D.; MacDougall, B. Infrared Spectroscopy on Size-controlled Synthesized Pt-Based Nano-Catalysts. *Surf. Sci.* **2006**, *600*, 3502-3511.

18. Neumann, S.; Grotheer, S.; Tielke, J.; Schrader, I.; Quinson, J.; Zana, A.; Oezaslan, M.; Arenz, M.; Kunz, S. Nanoparticles in a Box: a Concept to Isolate, Store and Re-Use Colloidal Surfactant-Free Precious Metal Nanoparticles. *J. Mater. Chem. A* **2017**, *5*, 6140-6145.

19. Speder, J.; Altmann, L.; Baumer, M.; Kirkensgaard, J. J. K.; Mortensen, K.; Arenz, M. The Particle Proximity Effect: from Model to High Surface Area Fuel Cell Catalysts. *RSC Adv.* **2014**, *4*, 14971-14978.

20. Strobel, R.; Stark, W. J.; Mädler, L.; Pratsinis, S. E.; Baiker, A. Flame-Made Platinum/Alumina: Structural Properties and Catalytic Behaviour in Enantioselective Hydrogenation. *J. Catal.* **2003**, *213*, 296-304.

21. Speder, J.; Zana, A.; Spanos, I.; Kirkensgaard, J. J. K.; Mortensen, K.; Hanzlik, M.; Arenz, M. Comparative Degradation Study of Carbon Supported Proton Exchange Membrane Fuel Cell Electrocatalysts - The Influence of the Platinum to Carbon Ratio on the Degradation Rate. *J. Power Sources* **2014**, *261*, 14-22.

22. Deutschmann, O.; Knözinger, H.; Kochloefl, K.; Turek, T. Heterogeneous Catalysis and Solid Catalysts. In *Ullmann's Encyclopedia of Industrial Chemistry*, Wiley: 2009.

23. Morsbach, E.; Brauns, E.; Kowalik, T.; Lang, W.; Kunz, S.; Baumer, M. Ligand-Stabilized Pt Nanoparticles (NPs) as Novel Materials for Catalytic Gas Sensing: Influence of the Ligand on Important Catalytic Properties. *Phys. Chem. Chem. Phys.* **2014**, *16*, 21243-21251.

24. Schrader, I.; Neumann, S.; Himstedt, R.; Zana, A.; Warneke, J.; Kunz, S. The Effect of Particle Size and Ligand Configuration on the Asymmetric Catalytic Properties of Proline-Functionalized Pt-Nanoparticles. *Chem. Commun.* **2015**, *51*, 16221-16224.

25. Speder, J.; Zana, A.; Arenz, M. The Colloidal Tool-Box Approach for Fuel Cell Catalysts: Systematic Study of Perfluorosulfonate-Ionomer Impregnation and Pt Loading. *Catal. Today* **2016**, *262*, 82-89.

26. Speder, J.; Zana, A.; Spanos, I.; Kirkensgaard, J. J. K.; Mortensen, K.; Arenz, M. On the Influence of the Pt to Carbon Ratio on the Degradation of High Surface Area Carbon Supported PEM Fuel Cell Electrocatalysts. *Electrochem. Commun.* **2013**, *34*, 153-156.

27. Schrader, I.; Warneke, J.; Neumann, S.; Grotheer, S.; Swane, A. A.; Kirkensgaard, J. J. K.; Arenz, M.; Kunz, S. Surface Chemistry of "Unprotected" Nanoparticles: A Spectroscopic Investigation on Colloidal Particles. *J. Phys. Chem. C* **2015**, *119*, 17655-17661.

28. Wang, Y. J.; Zhao, N. N.; Fang, B. Z.; Li, H.; Bi, X. T. T.; Wang, H. J. Effect of Different Solvent Ratio (Ethylene Glycol/Water) on the Preparation of Pt/C Catalyst and its Activity Toward Oxygen Reduction Reaction. *RSC Adv.* **2015**, *5*, 56570-56577.

29. Bock, C.; Paquet, C.; Couillard, M.; Botton, G. A.; MacDougall, B. R. Size-Selected Synthesis of PtRu Nano-Catalysts: Reaction and Size Control Mechanism. *J. Am. Chem. Soc.* **2004**, *126*, 8028-8037.

30. Li, X.; Chen, W. X.; Zhao, J.; Xing, W.; Xu, Z. D. Microwave Polyol Synthesis of Pt/CNTs Catalysts: Effects of pH on Particle Size and Electrocatalytic Activity for Methanol Electrooxidization. *Carbon* **2005**, *43*, 2168-2174.

31. Qiu, J. S.; Zhang, H. Z.; Liang, C. H.; Li, J. W.; Zhao, Z. B. Co/CNF Catalysts Tailored by Controlling the Deposition of Metal Colloids onto CNFs: Preparation and Catalytic Properties. *Chem. - Eur. J.* **2006**, *12*, 2147-2151.

32. Chu, Y. Y.; Wang, Z. B.; Gu, D. M.; Yin, G. P. Performance of Pt/C Catalysts Prepared by Microwave-Assisted Polyol Process for Methanol Electrooxidation. *J. Power Sources* **2010**, *195*, 1799-1804.

33. Kawasaki, H.; Kosaka, Y.; Myoujin, Y.; Narushima, T.; Yonezawa, T.; Arakawa, R. Microwave-Assisted Polyol Synthesis of Copper Nanocrystals without Using Additional Protective Agents. *Chem. Commun.* **2011**, *47*, 7740-7742.

34. He, B. L.; Chen, Y. X.; Liu, H. F.; Liu, Y. Synthesis of Solvent-Stabilized Colloidal Nanoparticles of Platinum, Rhodium, and Ruthenium by Microwave-Polyol Process. *J. Nanosci. Nanotechnol.* **2005**, *5*, 266-270.

35. Mayrhofer, K. J. J.; Blizanac, B. B.; Arenz, M.; Stamenkovic, V. R.; Ross, P. N.; Markovic, N. M. The Impact of Geometric and Surface Electronic Properties of Pt-Catalysts on the Particle Size Effect in Electocatalysis. *J. Phys. Chem. B* **2005**, *109*, 14433-14440.

36. Gasteiger, H. A.; Kocha, S. S.; Sompalli, B.; Wagner, F. T. Activity Benchmarks and Requirements for Pt, Pt-alloy, and non-Pt Oxygen Reduction Catalysts for PEMFCs. *Appl. Catal., B* **2005**, *56*, 9-35.

37. Li, D. G.; Wang, C.; Strmcnik, D. S.; Tripkovic, D. V.; Sun, X. L.; Kang, Y. J.; Chi, M. F.; Snyder, J. D.; van der Vliet, D.; Tsai, Y. F.; Stamenkovic, V. R.; Sun, S. H.; Markovic, N. M. Functional Links between Pt Single Crystal Morphology and Nanoparticles with Different Size and Shape: the Oxygen Reduction Reaction Case. *Energy Environ. Sci.* **2014**, *7*, 4061-4069.

612 38. Lv, H. F.; Li, D. G.; Strmcnik, D.; Paulikas, A. P.; Markovic, N. M.; Stamenkovic, V. R.
613 Recent advances in the design of tailored nanomaterials for efficient oxygen reduction reaction.
614 *Nano Energy* **2016,** *29*, 149-165.

615 39. Steinfeldt, N. In Situ Monitoring of Pt Nanoparticle Formation in Ethylene Glycol
616 Solution by SAXS-Influence of the NaOH to Pt Ratio. *Langmuir* **2012**, *28*, 13072-13079.

617 40. Calvin, S.; Miller, M. M.; Goswami, R.; Cheng, S. F.; Mulvaney, S. P.; Whitman, L. J.;
618 Harris, V. G. Determination of Crystallite Size in a Magnetic Nanocomposite Using Extended X-
619 ray Absorption Fine Structure. *J. Appl. Phys.* **2003**, *94*, 778-783.

620 41. MontejanoCarrizales, J. M.; AguileraGranja, F.; MoranLopez, J. L. Direct Enumeration
621 of the Geometrical Characteristics of Clusters. *Nanostruct. Mater.* **1997**, *8*, 269-287.

622 42. Billinge, S. J. L.; Kanatzidis, M. G. Beyond Crystallography: the Study of Disorder,
623 Nanocrystallinity and Crystallographically Challenged Materials with Pair Distribution
624 Functions. *Chem. Commun.* **2004**, 749-760.

625 43. Billinge, S. J. L.; Levin, I. The Problem with Determining Atomic Structure at the
626 Nanoscale. *Science* **2007**, *316*, 1698-1698.

627 44. Jensen, K. M. O.; Juhas, P.; Tofanelli, M. A.; Heinecke, C. L.; Vaughan, G.; Ackerson,
628 C. J.; Billinge, S. J. L. Polymorphism in Magic-sized $Au_{144}(SR)_{60}$ Clusters. *Nat. Commun.* **2016**,
629 *7*. DOI:10.1038/ncomms11859.

630 45. Leontyev, I. N.; Kuriganova, A. B.; Leontyev, N. G.; Hennet, L.; Rakhmatullin, A.;
631 Smirnova, N. V.; Dmitriev, V. Size Dependence of the Lattice Parameters of Carbon Supported

632 Platinum Nanoparticles: X-ray Diffraction Analysis and Theoretical Considerations. *RSC Adv.*
633 **2014**, *4*, 35959-35965.

634 46. Zhu, F. J.; Kim, J.; Tsao, K. C.; Zhang, J. L.; Yang, H. Recent Development in the
635 Preparation of Nanoparticles as Fuel Cell Catalysts. *Curr. Opin. Chem. Eng.* **2015**, *8*, 89-97.

636 47. Arenz, M.; Mayrhofer, K. J. J.; Stamenkovic, V.; Blizanac, B. B.; Tomoyuki, T.; Ross, P.
637 N.; Markovic, N. M. The Effect of the Particle Size on the Kinetics of CO Electrooxidation on
638 High Surface Area Pt Catalysts. *J. Am. Chem. Soc.* **2005**, *127*, 6819-6829.

639 48. Oh, H.-S.; Oh, J.-G.; Hong, Y.-G.; Kim, H. Investigation of carbon-supported Pt
640 nanocatalyst preparation by the polyol process for fuel cell applications. *Electrochim. Acta* **2007,**
641 *52* (25), 7278-7285.

642 49. Oh, H.-S.; Oh, J.-G.; Kim, H. Modification of Polyol Process for Synthesis of Highly
643 Platinum Loaded Platinum-Carbon Catalysts for Fuel Cells. *J. Power Sources* **2008**, *183*, 600-
644 603.

645 50. Nesselberger, M.; Ashton, S.; Meier, J. C.; Katsounaros, I.; Mayrhofer, K. J. J.; Arenz,
646 M. The Particle Size Effect on the Oxygen Reduction Reaction Activity of Pt Catalysts:
647 Influence of Electrolyte and Relation to Single Crystal Models. *J. Am. Chem. Soc.* **2011**, *133*,
648 17428-17433.

649 51. Inaba, M.; Quinson, J.; Arenz, M. pH matters: The Influence of the Catalyst Ink on the
650 Oxygen Reduction Activity Determined in Thin Film Rotating Disk Electrode Measurements. *J.*
651 *Power Sources* **2017**, *353*, 19-27.

52. Kacenauskaite, L.; Quinson, J.; Schultz, H.; Kirkensgaard, J. J. K.; Kunz, S.; Vosch, T.; Arenz, M. UV-Induced Synthesis and Stabilization of Surfactant-Free Colloidal Pt Nanoparticles with Controlled Particle Size in Ethylene Glycol. *ChemNanoMat* **2017**, *2*, 89-93.

53. Kacenauskaite, L.; Swane, A. A.; Kirkensgaard, J. J. K.; Fleige, M.; Kunz, S.; Vosch, T.; Arenz, M. Synthesis Mechanism and Influence of Light on Unprotected Platinum Nanoparticles Synthesis at Room Temperature. *ChemNanoMat* **2016**, *2*, 104-107.

54. Newville, M. IFEFFIT: Interactive XAFS Analysis and FEFF Fitting. *J. Synchrotron Radiat.* **2001**, *8*, 322-324.

55. Hammersley, A. P.; Svensson, S. O.; Hanfland, M.; Fitch, A. N.; Hausermann, D. Two-Dimensional Detector Software: From Real Detector to Idealised Image or Two-Theta Scan. *High Pressure Res.* **1996**, *14*, 235-248.

56. Yang, X.; Juhas, P.; Farrow, C. L.; Billinge, S. J. L. xPDFsuite: an End-to-End Software Solution for High Throughput Pair Distribution Function Transformation, Visualization and Analysis. *arXiv:1402.3163 [cond-mat.mtrl-sci]* **2015**.

57. Juhas, P.; Farrow, C. L.; Yang, X.; Knox, K. R.; Billinge, S. J. L. Complex Modeling: a Strategy and Software Program for Combining Multiple Information Sources to Solve Ill Posed Structure and Nanostructure Inverse Problems. *Acta Crystallogr., Sect. A: Found. Adv.* **2015**, *71*, 562-568.

673

674 TABLE OF CONTENTS

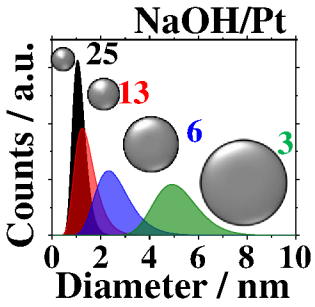

675

676

677

678

679

680